Electrodynamic characterisitcs measurements of higher order modes in S-band cavity

IOP Conf. Series: Journal of Physics: Conf. Series **941** (2017) 012089 doi:10.1088/1742-6596/941/1/012089

Electrodynamic characterisitcs measurements of higher order modes in S-band cavity

R Donetsky , M Lalayan, N P Sobenin, A Orlov and A Bulygin

National Research Nuclear University, "MEPhI", Moscow, Russia

E-mail: yvshashkov@mephi.ru

Abstract: The 800 MHz superconducting cavities with grooved beam pipes were suggested as one of the harmonic cavities design options for High Luminosity LHC project. Cavity simulations were carried out and scaled aluminium prototype having operational mode frequency of 2400 MHz was manufactured for testing the results of simulations. The experimental measurements of transverse shunt impedance with error estimation for higher order modes TM_{110} and TE_{111} for S-band elliptical cavity were done. The experiments using dielectric and metallic spherical beads and with ring probe were carried out. The Q-factor measurements for two-cell structure and array of two cells were carried out.

1. The influence of various factors on frequency and Q-factor measurement in the 2400 MHz prototype of superconducting harmonic cavity

Despite the high accuracy of modern electromagnetic field dispersion in cavities simulation software it is still necessary and important to manufacture a prototype of the structure under development in order to measure its electrodynamics characteristics (EDCs) of both operational and higher order modes [1-4]. In order to provide precise frequency f_0, Q-factor and shunt impedance measured values various factors should be taken into account, namely the specific pressure at the junction points of the sections, the surface roughness, the temperature and the immersion depth of the exciting and receiving RF pickups. This paper consists of three parts: the first one is devoted to the experiments analysis of the pressure, position and penetration of probes into the cavity influence. All measurements were made on the scaled 2400 MHz harmonic cavity model built for testing the damping efficiency of the method proposed for the High luminosity LHC project [5-8]. The second part presents the experimental and calculated field dispersion analysis results obtained by bead pull measurements. Results of the Q-factor measurements for the two cell cavity structure are presented in third section.

1.1. Pressure influence

Measurements were done with Vector network analyzer Agilent 8753ET. The modes of interest are TM_{010}, TE_{111} and TM_{110} (figure 1). Pickups used for modes excitation are shown on figure 2. The Q-values were measured by common 3 dB bandwidth method (1), where f_0 is the frequency of the mode and Δf is the bandwidth corresponding to -3 dB drop in transmission:

$$Q_L = f_0/\Delta f \quad (1)$$

The accuracy of the frequency measurements with analyser is less than 1 kHz resulting in precision of10^{-4} %.

In order to ensure the good contact between different parts of the model it was tested in the test bench equipped with hydraulic press. On figure 3 operational mode TM_{010} specific pressure on Q-factor dependency is presented, on figure 4 frequency dependency is presented. Saturation region can be found on the graph between the values of $\sigma = 160 \div 200$ kg/cm^2. All measurements were done at the pressure close to 180 kg/cm^2.

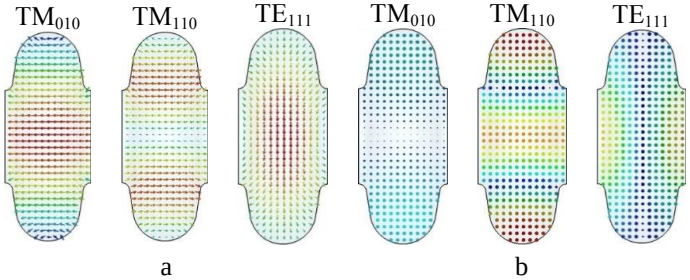

Figure. 1. Field dispersion of TM_{010}, TE_{111} and TM_{110} modes: (a) Electric field; (b) Magnetic field.

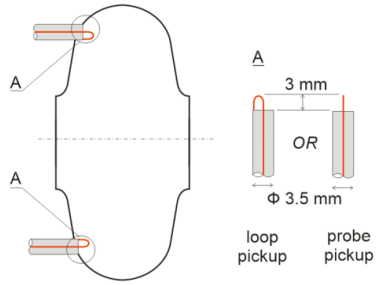

Figure. 2. Cavity with the location of the pickups.

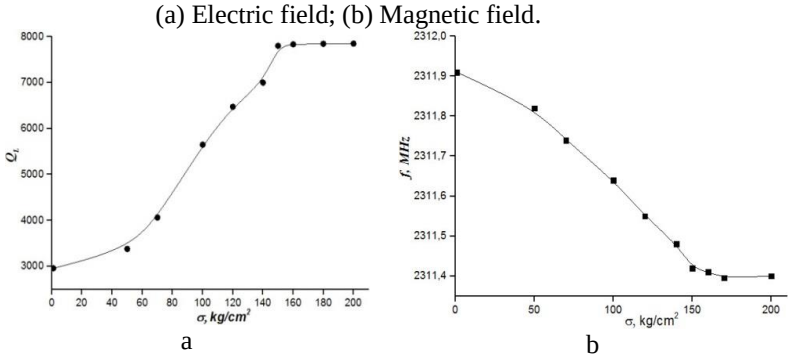

Figure. 3. TM_{010} mode Q-factor (a) and Frequency (b)vs. specific pressure.

.

1.2. Electric (probe) and magnetic (loop) pickups penetration depth influence

The influence of the probe penetration depth on f and Q_L was determined, as well as the dependence of the loaded Q-factor on the loop rotation angle with respect to its axis. Measurements were made for a loop and a probe. TM_{110} and TE_{111} modes are weakly excited by the probe. In the place where the probe is located it is not possible to create the necessary configuration of the electric field lines (figure 2). Therefore the electric probe was used for fundamental mode study whereas the loop pickup was used for dipole waves EDCs measurements. The loaded Q-factor measured using a loop features non-linear variation. So the influence of the loop rotation angle relative to the axis, on the loaded Q-factor was measured (figure 4).

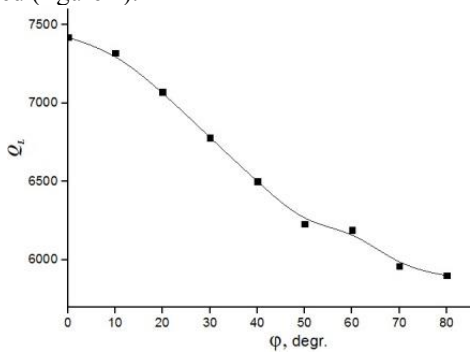

Figure. 4. Dependence of the loaded Q-factor on the loop rotation angle for TM_{010} (0° - the plane of the loop is perpendicular to the lines of the magnetic field).

The dependence shown on figure 5 is close to linear one with the slope coefficient of the straight line $\frac{Q_L}{\varphi} = 30\ \frac{1}{degree.}$. Figure 5 (a) illustrates the frequency f_0 dependence on the probe penetration depth l for TM_{010}, TM_{110} and TE_{111} modes at different locations of the probe (0 and 2 mm penetration depth). At Fig. 5b penetration depth dependence on Q_l is presented. Rotation angle precision is $\Delta\varphi = \pm 5^{\circ}$ resulting in $\Delta Q_L = \pm 150$ and the length depth $\Delta l = \pm 0{,}05$ mm. At figure 5 $\Delta f(l)$ and $Q_L(l)$ graphs taking into the account precision of the probe position are shown.

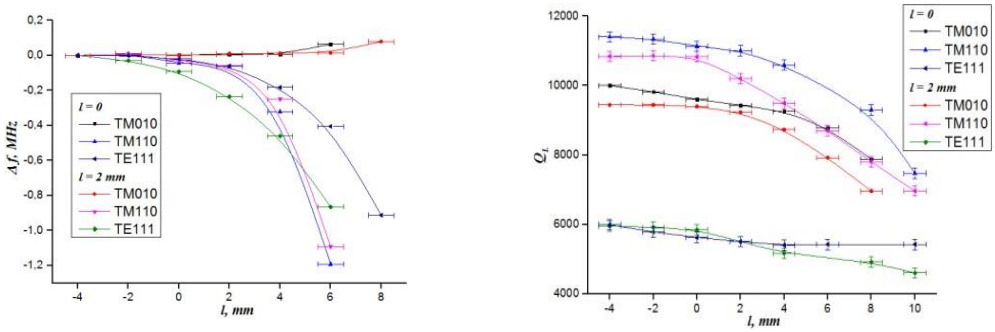

a b

Figure. 5. Dependences: $(a)\Delta f(l)$, (b) $Q_L(l)$.

Small perturbation theorem states that the perfectly conducting body introduced into the cavity could affect the frequency in two ways: first by disturbing the electric field and decreasing the cavity frequency, and second by disturbing the magnetic field leading to frequency increase. As it could be seen on Figure 5 the operational mode frequency increases with the introduction of a probe into the cavity, and the dipole waves frequency decreases. As a consequence of the theorem on small perturbations and from the dispersion of the electromagnetic field for the operational mode consideration, the probe interacts with magnetic field and with the electric field for the dipole waves. With decreasing of the coupling pickup penetration the external quality factor increases; in accordance with the known expression $\frac{1}{Q_L} = \frac{1}{Q_0} + \frac{1}{Q_{ext}}$ the measured loaded Q-factor will be closer to Q_0, which we compare with the simulation results. Table. 1 shows the values of the loaded Q-factors Q_L and the frequency of the modes under study with the minimal influence of the coupling elements.

Table 1. Results of the experiment and simulation

Mode	TM_{010}	TM_{110}	TE_{111}
Frequency, MHz (calculated)	2311,4	3457,0	4000,9
Frequency, MHz (measured)	2315,9	3455,7	4006,7
Q_0 (calculated)	13900	16500	16700
Q_l (measured)	10000 ± 200	11400 ± 230	6000 ± 120

2. Shunt impedance measurements in single cell 2400 MHz cavity

The transverse impedance $r_{\perp}/Q_0$ measurements could be done with two methods: direct integration of transverse magnetic H_{tr} and electric E_{tr} field components (2) and Panofsky-Wenzel theorem (3):

$$\frac{r_{sh\perp}}{Q_0} = \frac{\left| i \cdot c \cdot \mu_0 \int_0^l H_{tr}(z) \exp(ik_z z)\, dz - \int_0^l E_{tr}(z) \exp(ik_z z)\, dz \right|^2}{(\omega \cdot W) \cdot l} \quad (2)$$

$$\frac{r_{sh\perp}}{Q_0} = \frac{\left| \int_0^l \frac{\partial E_z(z)}{\partial z} \exp(ik_z z)\, dz \right|^2}{(\omega \cdot W) \cdot l} \quad (3)$$

where c is the speed of light, μ_0 is the magnetic constant, $k_z = 2\pi/\lambda$ is the longitudinal wave factor, $\omega = 2 \cdot \pi \cdot f$ is the wave frequency, W is the stored energy, l is the length of the structure.
The field distribution can be found using the perturbation theorem [9]:

$$\frac{\Delta f_{cs}(z)}{f_0} = -k_{c\perp}^{E}\frac{E_{tr}^2(z)}{W} - k_{c||}^{E}\frac{E_{tr}^2(z)}{W} \quad (4)$$

$$\frac{\Delta f_{ms}(z)}{f_0} = -k_{m\perp}^{E}\frac{E_{tr}^2(z)}{W} + k_{m\perp}^{H}\frac{H_{tr}^2(z)}{W} - k_{m||}^{E}\frac{E_z^2(z)}{W} + k_{m||}^{H}\frac{H_z^2(z)}{W} \quad (5)$$

$\Delta f_{cs}$and Δf_{ms} – are the frequency perturbation by ceramic and metal beads, k – transverse or longitudinal form factor for electric or magnetic field.

The electric field component can be easily measured by the ceramic bead because they do not perturb magnetic field. The magnetic field can be obtained as a difference between measurement results with metal and ceramic beads. The simulations were done for several perturbing beads in order to define the optimal combination of bodies to establish the most precise values of $r_{sh\perp}/Q_0$. Form factor values for different beads are presented in Table 2.

Table 2. Formfactors of the perturbing beads

Formfactor	ceramic sphere	metal sphere	metal ring
$k_{\perp}^{E} \cdot 10^{-20}$, m^2s/Ohm	1,97±0,02	2,32±0,03	1.92
$k_{||}^{E} \cdot 10^{-20}$, m^2s/Ohm	1,97±0,02	2,32±0,03	0.09
$k_{\perp}^{H} \cdot 10^{-15}$, m^2 ·s·Ohm	NA	1,73±0,03	1.36
$k_{||}^{H} \cdot 10^{-15}$, m^2 ·s·Ohm	NA	1,73±0,03	0.01

While evaluating the measurement results the frequency, Q-factor and phase measurement error, bead form factor uncertainty and bead off-axis misalignment were taken into account. The total measurement uncertainty lies well below 8% of those bead off-axis misalignment introduces the most contribution. The simulation and measurement results of $\Delta f/f_0$ are presented in figure 6. The comparison of measured and simulated field distribution of field components presented in figure 7.

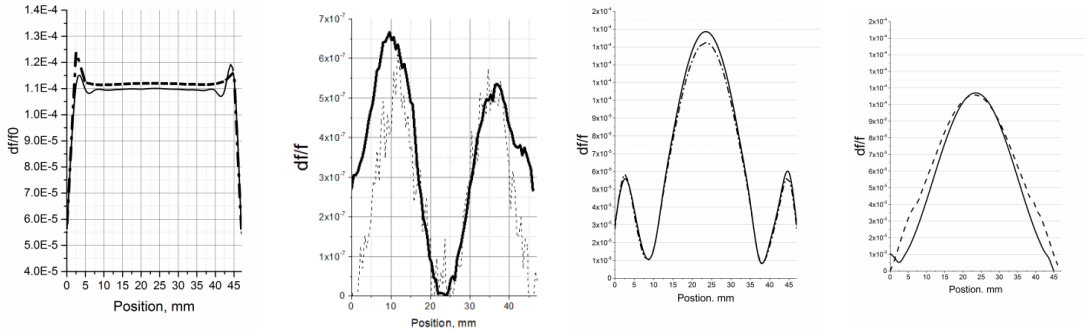

a b c d

Figure 6. $\Delta f/f_0$for metal sphere and ceramic sphere for TM_{110} (a,b) and TE_{111} (c,d). Straight line – measurements, dotted – simulations.

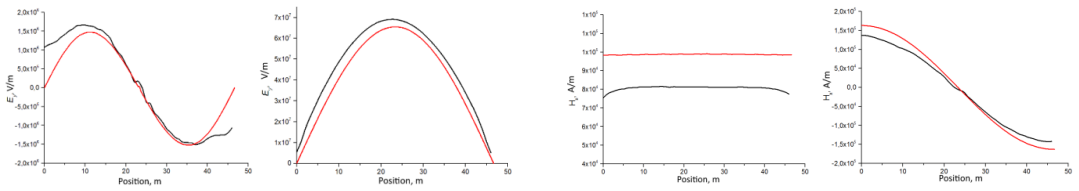

a b

Figure 7. (a) Magnetic and (b) Electric field distributions for ring bead for TE_{111} and TM_{110}. Red – simulation, black – measurements.

Shunt impedance values obtained experimentally using two methods mentioned above (namely Panofsky-Wenzel referred as P.-W. hereafter and direct integration one) are summarized in Table 3. As one could see all these results agree well.

Table 3. $r_{sh\perp}/Q$ simulation and measurements results on TM_{110} and TE_{111} modes

Mode	TM_{110}	TE_{111}	
		MS+CS	MR+CS
Simulation (direct integration)	985	43,4	
Simulation (P.-W.)	985	42,9	
Measurements (direct integration)	788	35,4	48,2
Measurements (P.-W.)	717	32,9	NA

3. Q-factor measurements for two-cell and array of cells structure

The 800 MHz superconducting cavities with grooved beam pipes were suggested as one of the harmonic cavities design options [10] for HL-LHC project. Simulations showed that it is possible to achieve Q-factor values in a structure with grooved beam pipe lower than 100 for the most dangerous dipole modes and 1000 for modes with higher frequency. The results obtained in Multi-P program [11] showed that this structure is free of multipacting discharge [12].

Q-factor measurements were made for a structure consisting of two cells connected by a narrow drift tube and two corrugated tubes at the sides (figure 8). Q-factor measurements were also made for two-cell cavity with corrugated drift tube (figure 9) which might be an interesting option for Future circular collider . To reduce the Q-value of dangerous dipole HOMs, damping ferrite rings were added at the ends of the drift tubes. Figure 10 presents the results of an experiment on loaded Q measurement in a structure with ferrite rings and without rings.

The damped Q-factor for most of HOMs is less than 1000, except for a few modes indicated by the numbers on the chart. However, those HOMs have low R/Q values and therefore could be treated as inessential with respect to their influence on beam dynamics. All other HOMs were damped well below the sensitivity of the analyzer. The fundamental mode loaded quality factor after damping changed insignificantly.

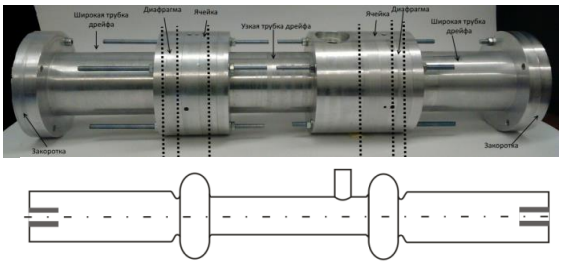

Figure 8. Two separated cells structure with corrugated beam pipes.

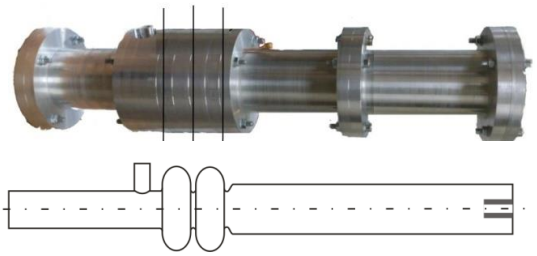

Figure 9. Two-cell cavity with corrugated beam pipe.

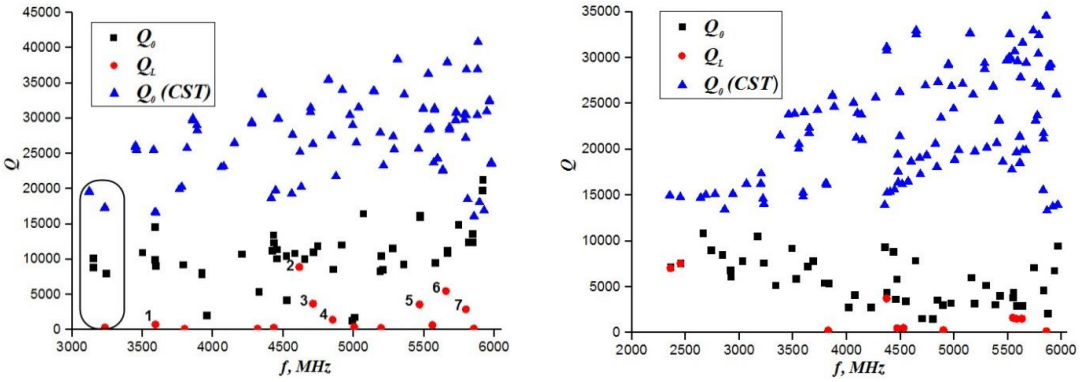

a b

Figure 10. Q values for (a) two cells separated by beam pipe; (b) two-cell cavity with drift tubes connected. Blue – Q-factor without damping ferrite rings in the drift tube, red - Q-factor with ferrite rings. 1 – dipole mode trapped in beam pipe between cells; 2,3,4 – quadrupole HOMs; 5,6,7 – sextupole HOMs.

Conclusion

The field dispersions obtained with bead pull measurements as well as measurements of transverse shunt impedance for higher order modes TM_{110} and TE_{111} for S-band elliptical cavity are in a good convergence with simulation results. For the manufactured two-cell and array of two cells aluminium prototypes results of loaded Q-factor measurements of higher order modes are also agree with a simulation results.

This project is supported in part by the MEPhI 5/100 Program of the Russian Academic Excellence Project.

References

[1] Navarro-Tapia M and Calaga R 2015 Bead-pull measurements of the main deflecting mode of the double quarter-wave cavity for the HL-LHC *Proceedings of 17th International Conference on RF Superconductivity (SRF2015): Whistler, Canada, September 13-18, 2015,* p. 1105-1109

[2] Hahn H and Calaga R, Jain P, Johnson E C, and Xu W 2014 HOM identification by bead pulling in the Brookhaven ERL cavity, Nucl. Instrum. Methods Phys. Res., Sect. A 734, 72 (2014)

[3] Zavadtsev A A , Zavadtsev D A , Nikolskiy K I , Savin E A and Sobenin N P 2013 Design and tuning of a 40-MeV electron linear accelerator Instrum. Exp. Tech. 2013; 56(5), pp. 506-515

[4] Savin E A, Matsievskiy S, Shashkov Ya V, Sobenin N P and Zavadtsev A A 2014 Multi-bunch generator cavity, Proceedings of the 5th International Particle Accelerator Conference, pp. 2267-2269

[5] Shashkov Ya V, Sobenin N P, Gusarova M A, Lalayan M V, Bazyl D S, Donetskiy R V, Orlov A I, Zobov M M and Zavadtsev A A 2016 Measurement of electrodynamics characteristics of higher order modes for harmonic cavity at 2400 MHz, Journal of Physics: Conference Series, Volume 747, Number 1

[6] Shashkov Ya V, Sobenin N P, Petrushina I I and Zobov M M 2014 Comparison of higher order modes damping techniques for 800 MHz single cell superconducting cavities, Nuclear Instruments and Methods in Physics Research A, v. Volume 767, pp. 271–280

[7] Shashkov Ya V, Sobenin N P and Zobov M M 2014 Comparison of High Order Modes damping techniques for 800 mhz single cell superconducting cavities Proc. IPAC'14,

Dresden, Germany (2014) pp 2258-2261
[8] Ya. V. Shashkov, A.A. Mitrofanov, N.P. Sobenin, V.L. Zvyagintsev, Analysis of higher order modes damping techniques in 9 cell cavity with modified drift tubes, Journal of Physics: Conference Series, Volume 74, p. 124-131
[9] B.V. Zverev B V and Sobenin N P 1993 Electrodynamic Characteristics of Accelerating Cavities Energoatomizdat, Moscow
[10] Shashkov YaV, Sobenin N P, Bazyl D S, Kaminskiy V I, Mitrofanov A A, Zobov M, 2016 Suppression of higher order modes in an array of cavities using waveguides, Journal of Physics: Conference Series, Volume 74, p. 116-123
[11] Gusarova M, Khudyakov S, Petrushina I I and Shashkov Ya V 2014 New Possibilities of MultP-M Code Proc. IPAC'14, Dresden, Germany (2014), pp 433-435
[12] Petrushina I I and Gusarova M A 2014 Multipactor in elliptical cavities 800 MHz Proceedings of 24th Russian Particle Accelerator Conference 2014, pp. 365-367